Environ Earth Sci (2009) 59:901–911
DOI 10.1007/s12665-009-0085-6

ORIGINAL ARTICLE

Experimental study on imbibition displacement mechanisms of two-phase fluid using micro model

Liang-Cheng Chang · Jui-Pin Tsai · Hsin-Yu Shan · Hung-Hui Chen

Received: 11 March 2008 / Accepted: 29 January 2009 / Published online: 20 February 2009

Abstract This study applies a transparent micro model and digital image analysis to the experimental study of the displacement mechanisms for water and air in porous media during imbibition process, and examines the displacement formulas. This study conducts experiments following Lenormand's assumptions as closely as possible. Various displacement mechanisms were observed, and their images were recorded. The displacement mechanisms in imbibition are mainly snap-off, In type imbibition and piston-type motion. The experimental fluid displacement images and associated capillary pressure were then used to verify the displacement formulas. This experimental study shows that, when snap-off occurred, the experimental capillary pressures were close to the Lenormand's estimation of critical capillary pressures where enough surrounding area of the throat was saturated. When I1 and I2 type imbibitions occurred, the experimental capillary pressures were also close to the Lenormand's estimation of critical capillary pressures where enough connecting throats were saturated. The In type imbibition and its associated piston-type motions are the main processes to increase the wetting phase fluid saturation. For the pore–throat distribution applied in this study, snap-off can facilitate the occurrence of In type imbibition and its associated piston-type motion; therefore, snap-off is an important displacement mechanism in facilitating the increase of the wetting phase fluid saturation in the imbibition process. To summarize, this study provides valuable experimental support and suggestions for Lenormand's displacement formulas, which are the basis for many related experimental and numerical studies.

Keywords Displacement mechanisms · Micro model · Imbibition · Porous media · Pore–throat network · Two-phase flow · Pore scale

List of symbols

θ	Contact angle
α	Half-corner (angle)
P	Pressure (cmH_2O)
S	Saturation (fraction)
P_c	Capillary pressure (cmH_2O)
P_{ce}	Experimental capillary pressure (cmH_2O)
$P_{snap\text{-}off1}$	Critical snap-off capillary pressure calculated by Hughes's formula
$P_{snap\text{-}off2}$	Critical snap-off capillary pressure calculated by Lenormand's formula
P_{In}	Critical In imbibition capillary pressure calculated by Lenormand's formula
S_w	Saturation of wetting phase fluid fraction
S_{nw}	Saturation of non-wetting phase fluid fraction
Sn_i.j	Sn indicated 'Snap-off where *i* is the throat label and *j* is the snap-off selected evolution step'
In_i.j	In indicated 'In type imbibitions' where *i* is the pore label and *j* is the In type imbibition selected evolution step

L.-C. Chang (✉) · J.-P. Tsai · H.-Y. Shan
Department of the Civil Engineering,
National Chiao Tung University, Hsin-chu, Taiwan
e-mail: lcchang@chang.cv.nctu.edu.tw

J.-P. Tsai
e-mail: skysky2cie@gmail.com; scorpio@chang.cv.nctu.edu.tw

H.-Y. Shan
e-mail: hyshan@mail.nctu.edu.tw

H.-H. Chen
Civil Engineering Department,
Min Hsin University Science Technology,
Hsin-chu, Taiwan
e-mail: chf@chang.cv.nctu.edu.tw

Introduction

Displacement mechanisms for two immiscible fluids in porous media are very important for groundwater hydrology and remediation as well as reservoir engineering. Capillary pressure is one of the most important forces in describing such a displacement mechanism. Researchers have studied the effect of capillary pressure on two-phase flow in porous media for more than three decades. (Dodd and Kiel 1959; Wardlaw and Taylor 1976). Lenormand et al. (1983), Lenormand and Zarcone (1984b) used displacement mechanisms to describe the relationship between capillary pressure and the interface curvature of two immiscible fluids. They examined the microscopic displacement mechanisms of water and air in porous media and proposed displacement formulas including 'In' type imbibitions that have been widely adapted to other analytical and simulation studies. Their displacement formula derivation assumes that the pore shape is square and the pore size is the same as its connecting throats. They also performed experiments to verify the formulas using a micro model with a pore–throat connected structure that had seven different throat sizes. However, the shape of pores in their micro model is irregular, and not fully consistent with the assumption of the displacement formula derivation.

A multi-phase flow in a pore–throat micro model with internal corners produces a thin film of wetting phase fluid in the corners for both drainage and imbibition processes. Lenormand et al. (1983) found that during the drainage process, the non-wetting phase fluid invades pores or throats that filled with wetting phase fluid. However, a thin film of wetting phase fluid remains in the extreme corner of the pore or throats. Thus, the wetting phase fluid in the corners forms a connected path even in the drainage process, and the disconnected wetting phase residual can leave the micro model through the connected path. In imbibition, the wetting phase fluid flows into the micro model via the continuous path and is therefore called "corner flow." The corner flow becomes thicker as capillary pressure decreases. When the capillary pressure decreases to the critical pressure of the displacement mechanisms, the wetting phase fluid does not contact the wall of the pore or throat. The interface of the two immiscible fluids collapses, and the wetting phase fluid fills the pore or throat. Therefore, the corners are the key to the displacement mechanism in a pore-throat network (Li and Wardlaw 1986; Hughes and Blunt 2000; Mahmud and Nguyen 2006). The critical capillary pressure depends on the size of the pore and throat, and the displacement is called In type imbibition or snap-off for pore and throat, respectively. Li and Wardlaw 1986, Mogensen and Stenby 1998 also pointed out that the occurrence of imbibition displacements in rectangular pore–throat micro model is more likely than in a circular model because of its corners.

Researchers have also performed 3-D pore scale modeling to study the curve characteristics of two phases flow in porous media based on a hypothetical 3-D pore–throat micro model (Jerauld and Salter 1990; Reeves 1997; Ioannidis and Chatzis 1993; Kawanishi et al. 1998; Mogensen and Stenby 1998; Vidales et al. 1998; Hughes and Blunt 2000; Mahmud and Nguyen 2006). As indicated previously, corners are important factors for pore–throat micro models. For a 3-D pore–throat micro model, a pore or throat with a circular cross section has no corner. Therefore, if a 3-D pore–throat micro model has either sphere pores or throats with circular cross sections, that micro model has no connected corner inside (Jerauld and Salter 1990 and Reeves 1997) and some of the displacement mechanisms cannot occur realistically. On the other hand, a 3-D pore or throat that has a non-circular (i.e., rectangular or triangular) cross section has corners. A pore–throat structure with pores and throats that has a non-circular cross section has connected corners inside (Ioannidis and Chatzis 1993; Kawanishi et al. 1998; Mogensen and Stenby 1998; Vidales et al. 1998; Hughes and Blunt 2000; Mahmud and Nguyen 2006). Because wetting phase fluid can flow into a pore–throat structure via the corners, all of the displacement mechanisms, such as snap-off and In type imbibitions, can occur when the capillary pressure decreases during the imbibition process. Therefore, a pore–throat micro model with a non-circular cross section is more realistic.

Due to difficulties in implementing 3-D micro model experiments, researchers often adapt the theories of displacement mechanisms for a 3-D pore scale network modeling from the results of 2-D micro model experimental studies (Lenormand et al. 1983; Lenormand and Zarcone 1984b; Li and Wardlaw 1986; Ioannidis et al. 1991). In fact, a 2-D micro model is simply a single layer 3-D micro model with a constant thickness layer. As stated previously, a 3-D pore–throat micro model without a circular cross section (Ioannidis and Chatzis 1993; Mogensen and Stenby 1998; Vidales et al. 1998; Hughes and Blunt 2000; Mahmud and Nguyen 2006) can realize all of the displacement mechanisms. The geometrically similar 2-D counterpart of a 3-D pore–throat micro model is a 2-D pore–throat micro model with square pores (Lenormand et al. 1983; Lenormand and Zarcone 1984b). Snap-off equations in a 2-D micro model can be directly applied to a 3-D micro model because they share the same mechanism. However, the In type imbibitions equations must be modified because the number of throats connected to a pore in 2-D and 3-D micro models is different (Blunt 1997; Hughes and Blunt 2000; Mahmud and Nguyen 2006).

Lenormand et al. (1983) and Lenormand and Zarcone (1984b) conducted some of the most significant 2-D micro model experimental studies. They derived displacement equations that were widely applied to other studies. However, the pores shape in their micro model was irregular, and not fully consistent with their assumption on deriving displacement formulas. Therefore, this study performs 2-D pore–throat micro model experiments with square pores to investigate the applicability of the displacement formulas. This study provides experimental support and modification suggestions to Lenormand's displacement formulas, and is a valuable reference for studying displacement mechanisms in porous media.

Related theory

Snap-off

During the imbibition process, the snap-off displacement mechanism only occurs in a throat. As the capillary pressure decreases, the wetting phase enters the transparent micro model through the continuous corner path. The interface of the two fluids thus changes its curvature, and the volume of the wetting phase (corner flow) increases at the throat and pore corner. As the capillary pressure reaches the critical capillary pressure where snap-off occurs, the interface collapses. The wetting phase fluid then occupies the throat and forces the non-wetting phase into the pores. This process is called snap-off (Lenormand et al. 1983; Lenormand and Zarcone 1984b). Lenormand and Zarcone (1984b) proposed the following equation to estimate the capillary pressure necessary for snap-off to occur,

$$\frac{P_{\text{snap-off1}}}{\gamma} = \frac{2(\cos\theta - \sin\theta)}{d} \tag{1}$$

where γ is interfacial tension, d is the width of the throat and θ is contact angle.

Hughes (1998) proposed the following equation to estimate the critical capillary pressure for snap-off to occur under the condition that the sum of the contact angle θ and the half-corner angle α is less than 90°,

$$P_{\text{snap-off2}} = \frac{\gamma}{r_1}(\cos\theta - \sin\theta\tan\alpha) \tag{2}$$

where γ is interfacial tension and r_t is the inscribed radius of the throat.

In type imbibition

During the imbibition process, the fluid displacement occurring in a pore is called In type imbibition (Lenormand et al. 1983; Lenormand and Zarcone 1984b) and the sub-index n is the number of throats surrounding a pore that fill with non-wetting phase fluid. Lenormand et al. (1983), Lenormand and Zarcone (1984b) illustrated the critical condition for I1 and I2 type imbibition to occur in a rectangular section. In I1 type imbibition, before wetting the pore with wetting phase fluid, only one throat surrounding the pore is filled with non-wetting phase fluid. The other neighboring throats are filled with wetting phase fluid. In I2 type imbibition, before wetting the pore with wetting phase fluid, two neighboring throats of the pore are filled with non-wetting phase fluid. The other neighboring throats are filled with wetting phase fluid. Lenormand and Zarcone (1984b) proposed an equation to estimate the capillary pressure required for I1 type imbibition to occur.

$$\frac{P_{11}}{\gamma} = \frac{\sqrt{2}}{d} + \frac{2\cos\theta}{x} \tag{3}$$

The critical capillary pressure for I2 type imbibition to occur can be estimated by the following equation:

$$\frac{P_{12}}{\gamma} = \frac{\cos\theta}{d} - \frac{1}{\sqrt{2}d} + \frac{2\cos\theta}{x} \tag{4}$$

Research procedure

Figure 1 shows the research procedure of this study. The fluid-pairs in this experimental research were air and water. As Fig. 1 shows, Step 1 is to perform the micro model experiments and record all the experimental images using a digital camera. A series of images were recorded for each stage of capillary head variation. The following section describes details of the experiment procedure. Step 2 is to analyze the impact of various fluid displacements on the saturation variation, and examine the accuracy of Lenormand's displacement theory based on the recorded images. For each stage of capillary head variation, the total saturation variation was obtained by comparing the last image of the stage to the starting image. Moreover, this study examines the series of images within each stage and obtains images associated with each fluid displacement. The saturation variations induced by the fluid displacements were then obtained by processing the selected images. For each stage of capillary pressure variation, the ratio of saturation variation for each fluid displacement to the total saturation variation can then be computed. Lenormand's displacement theory can predict the occurrence of various types of fluid displacement and compute the associated critical capillary pressure based on the fluid properties and porous structure. Therefore, the selected images can also be used to examine the occurrence of fluid displacement predicted by Lenormand's displacement theory.

Experimental design

Experiment system

The experimental system for P_c–S (capillary pressure–saturation) experiments (see Fig. 2) consists of a transparent acrylic micro model, head control sub-system, CCD camera, and light source. The head control sub-system includes connecting tubes and glass containers (reservoirs) whose elevations can be freely adjusted to control the heads. The two sides of the micro model are connected to the inflow and outflow reservoirs, respectively. A CCD camera recorded images of the fluid distribution in the micro model during the experiment. The P_c–S experiment is basically a static experiment. The fluids are static at the end of each stage of the experiment, and the degree of saturation for each phase varies according to the capillary pressure.

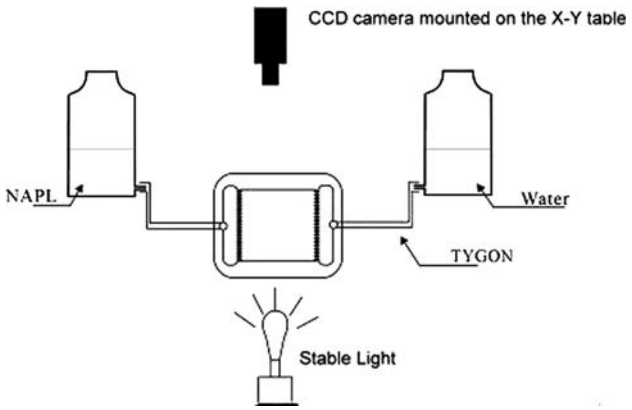

Fig. 2 Schematic diagram of the experimental setup for P_c–S curves

Micro model

The micro model is the most important component of this experimental system. Figure 3 shows the schematic diagram of the micro model for P_c–S experiments. The micro model consists of 25 pores and 40 throats. The pores and throats were connected to each other with a grid pattern, as the figure shows. Figure 3 shows the details of the pore and throat connection. The distance between the centers of two adjacent pores is 2.2 mm. For each pore and throat, the widths were randomly selected from five predetermined sizes using a Visual Basic Application (VBA) in AUTOCAD. Table 1 lists the widths and numbers of the pores and throats obtained in this study. The equivalent radii of the pores and throats in Table 1 were calculated according to geometric relation with the following Eq. 5,

$$\frac{1}{R} = \frac{1}{w} + \frac{1}{d} \tag{5}$$

Fig. 1 Research procedure

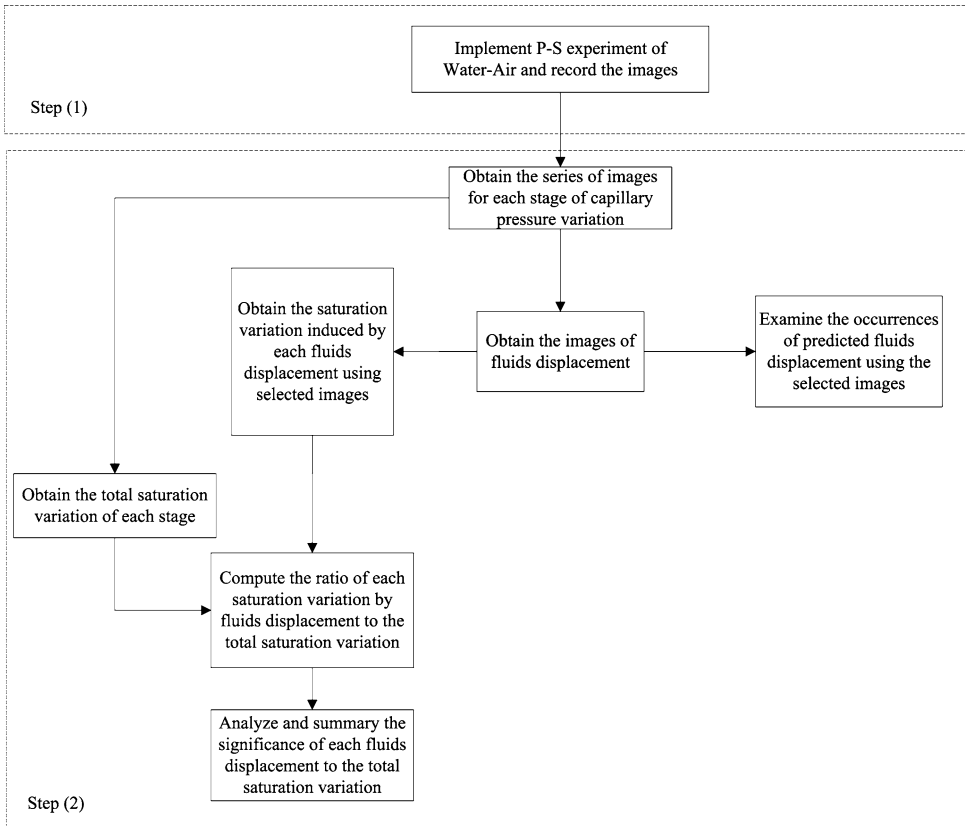

where R is the equivalent radius of the pores or throats, w is the width of pores or throats, and d is the depth. All pores and throats in the micro model are 0.8-mm deep. Table 1 shows the equivalent radii of the pores and throats for the micro model. For the P_c–S micro model, barriers were required to confine the non-wetting phase fluid within the micro model during experiment. Figure 3 shows that the barrier located at the boundary of the wetting phase fluid reservoir prevented the non-wetting phase fluid from leaking into the wetting phase fluid reservoir. The barriers consisted of many parallel micro-channels. The narrow width of the micro-channel created a condition where the capillary pressure at the micro-channel must be greater than the 'entry pressure' for the non-wetting phase fluid to pass through the barrier. Therefore, the width of the micro-channels was less than the minimal width of the pores or throats in the micro model. Each micro-channel in the barrier is 0.1 mm wide. The dark color in Fig. 3 shows the pores and throats with varied sizes in the micro model.

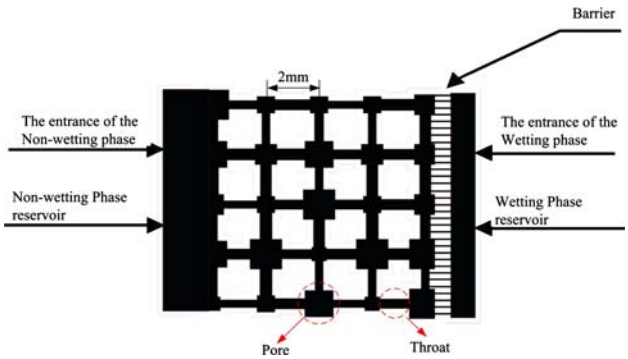

Fig. 3 Schematic diagram of micro model for displacement mechanisms

Table 1 The sizes and numbers of pores and throats

Width (mm)	Effective radius (mm)	Numbers	Occupied ratio
Pore			
0.60	0.343	3	0.011
0.72	0.379	6	0.034
0.88	0.419	6	0.046
1.14	0.470	4	0.051
1.28	0.492	6	0.097
Throat			
0.34	0.239	10	0.023
0.38	0.258	4	0.022
0.42	0.275	7	0.065
0.46	0.292	12	0.035
0.50	0.308	7	0.050

Depth = 0.8 mm

The acrylic surface of micro model is hydrophobic, and unlike the wetting condition of the soil particle surface in general. Chang et al. (2008) coated the micro model with silicate ($SiO_2 \bullet nNa_2O \bullet xH_2O, n = 2 \sim 4$) to make its surface into hydrophilic. This study follows their method to change the wetting characteristic of micro model into hydrophilic.

CCD camera

The CCD camera in this study was mounted on an x-y table above the micro model. The camera could move freely in all directions. The images were recorded in digital signals and stored in a personal computer. The CCD images were recorded at a resolution of 640 × 480 pixels, and each pixel was represented in RGB format. Throughout the experiment, the CCD camera recorded images at a time interval of 30 s. The recorded RGB images were examined using Adobe Photoshop software to determine the degree of saturation for both wetting and non-wetting phase fluids.

Experimental fluids

Air and water represent the non-wetting phase and wetting phase, respectively, in this study. The experimental fluids were dyed with different color to enhance visual observations and facilitate image analysis of their saturation in the micro model. De-ionized water was dyed blue, and the air naturally appeared white without dyeing. Since the concentration of the dye in the liquid was less than 0.05%, the dye had a minimal impact on the results of P_c–S experiments. Table 2 lists the properties of the liquids.

Experiment procedure

The temperature of the experiment in this study was maintained at 24°C. The following section provides a detailed description of the experiment.

Figure 4 shows the P_c–S experiment procedure. The micro model was saturated with wetting phase fluid before the experiment began. The experimental procedure contained two major stages: the drainage process and the imbibition process. During the drainage process, the capillary pressure increased step by step. The increase of capillary pressure for each step was equivalent to 0.1–0.4

Table 2 Physical property of the related fluids

Experimental fluids	Chemical formula	Density (g/cm^3) (24°C)	Surface tension (Dynes/cm)
Water	H_2O	0.997	71.5

cm of water head. The capillary pressure can be increased by either increasing the pressure head of the non-wetting phase fluid or decreasing the pressure head of wetting phase fluid. Both approaches can be implemented by adjusting the reservoir elevation. For each step, fluid distribution images were continuously recorded at 30-s intervals until the images showed no change for 30 min. The last image was then used to determine the fluid saturation associated with the capillary pressure. The drainage process experiment terminated when the capillary pressure nearly equaled the entry pressure of the barrier. The imbibition process was similar to the drainage process except that the capillary pressure decreased in steps.

All images were recorded by a CCD camera at a 640 × 480 pixel resolution, and each pixel was represented by R-G-B values. The images were examined using Adobe Photoshop software to determine the saturation of wetting phase fluids for each image. The saturation of the non-wetting phase can then be calculated.

Results and discussion

Examining the recorded images clearly shows the details of the fluid displacement, and its associated experimental capillary pressure was then compared with the estimated critical capillary pressure to verify the accuracy of

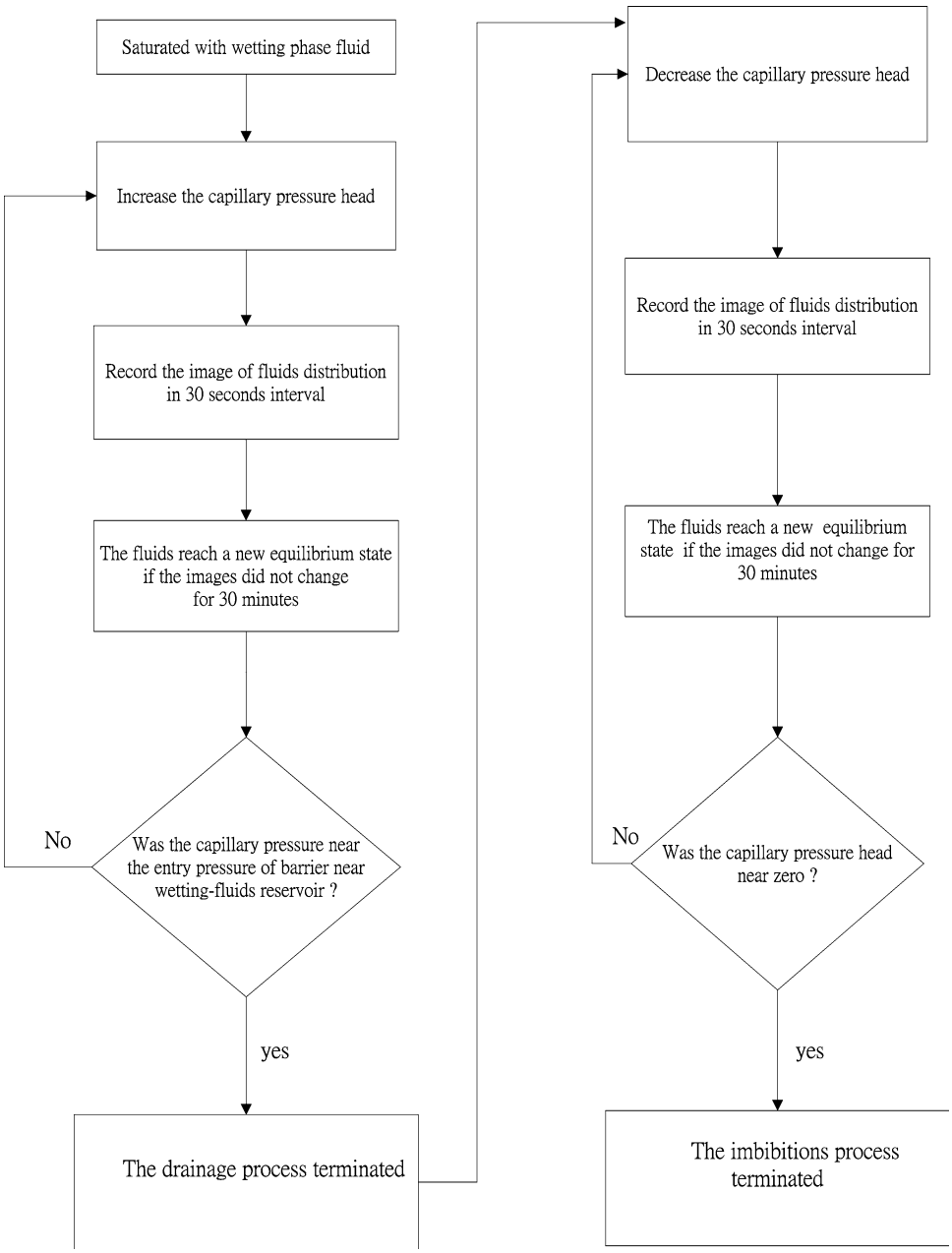

Fig. 4 Experimental procedure

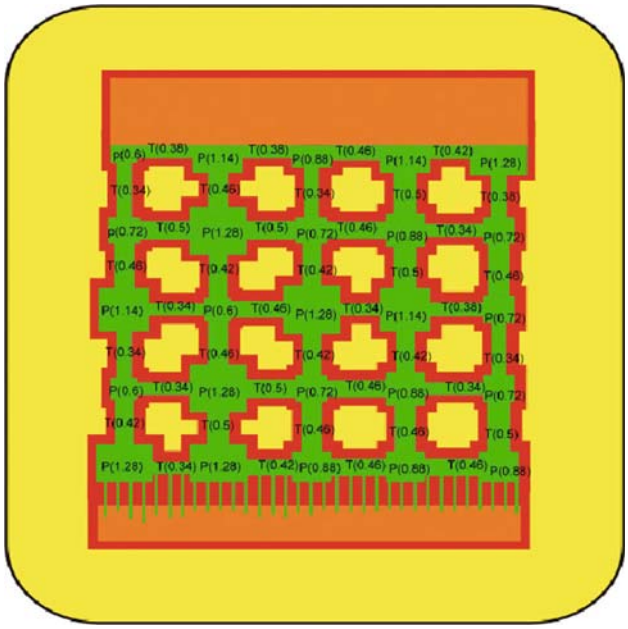

Fig. 5 The widths of pores and throats in the transparent micro model

Lenormand's formulas. Since the fluid displacement in the imbibition process was more complicated than that in drainage process, this section focuses on the imbibition process. To facilitate the discussion, Fig. 5 shows the dimensions of the pores and throats in the transparent micro model. In this figure, "T" indicates a throat, "P" indicates a pore, and the Arabic numerals give their associated dimensions.

Table 3 summarizes the critical capillary pressure as estimated by Lenormand's and Hughes's formulas, assuming the wettability is perfect ($\theta = 0°$) and the half-corner angle α equals 45° (the corner angle of the rectangular cross section of pores and throats was 90°). Using the series of recorded images, the following section compares these predicted values with the experimental capillary pressure alone.

Figure 6a–d shows the selected images in the 12th stage of the imbibition process, where P_{ce} equals 3.4 cmH_2O. The circled areas in the images demonstrate the detailed snap-off process at selected throats labeled with 'Sn_i.j', where i is the throat label and j is the selected snap-off evolution step. Figure 6a is the starting image of the snap-off process, and the widths of the selected throats 'Sn_1.0' and 'Sn_2.0' are 0.42 and 0.46 mm, respectively. Their computed $P_{snap\text{-}off1}$ are 2.53 and 2.39 cmH_2O, and $P_{snap\text{-}off2}$ are 3.48 and 3.18 cmH_2O. The $P_{snap\text{-}off1}$ for 'Sn_1.j' and 'Sn_2.j' are 0.87 and 0.97 cmH_2O lower than P_{ce}, respectively. The $P_{snap\text{-}off2}$ is 0.08 cmH_2O greater than P_{ce} for 'Sn_1.j' and 0.22 cmH_2O lower than P_{ce} for 'Sn_2.j'. This difference indicates that the critical snap-off capillary pressure as estimated by Lenormand's formula is closer to the P_{ce}.

Figure 6a shows that there were two fully wet throats and one partially wet throat close to 'Sn_1.0' in the beginning, and two fully wet throats neighboring 'Sn_2.0'. Figure 6b shows a selected image for the step after Fig. 6a. The 'Sn_1.1' and 'Sn_2.1' indicate the progress of the snap-off process at the same throats for 'Sn_1.0' and 'Sn_2.0'. The color changes in the figures indicate the wetting phase fluid invading through corner flow since the throats were not directly connected with other saturated pore or throats. Figure 6c is a selected image of the step after Fig. 6b. Sn_2.2 shows that the snap-off process for the throat is almost completed. Figure 6d indicates that the snap-off process is complete at 'Sn_1.3'. The snap-off progress shown at the two selected throats in the previous figures imply the existence of corner flow since both throats were not directly connecting to other fully wet pores or throats in the beginning. Moreover, the wetting of the two throats creates an environment for the occurrence of In type imbibition in the 14th stage.

Table 3 The estimated critical capillary pressure of various fluid displacements for the micro model's pores and throats in imbibition

Width (cm)	Snap-off1 (Hughes) (cmH_2O)	Snap-off2 (Lenormand) (cmH_2O)	I1 type imbibition (Lenormand) (cmH_2O)	I2 type imbibition (Lenormand) (cmH_2O)
Throat				
0.034	3.06	4.30	*	*
0.038	2.84	3.85	*	*
0.042	2.65	3.48	*	*
0.046	2.50	3.18	*	*
0.050	2.38	2.92	*	*
Pore				
0.060	*	*	3.53	2.19
0.072	*	*	3.24	2.13
0.088	*	*	2.98	2.08
0.114	*	*	2.72	2.02
0.128	*	*	2.62	2.00

* indicates that displacement mechanisms do not occur

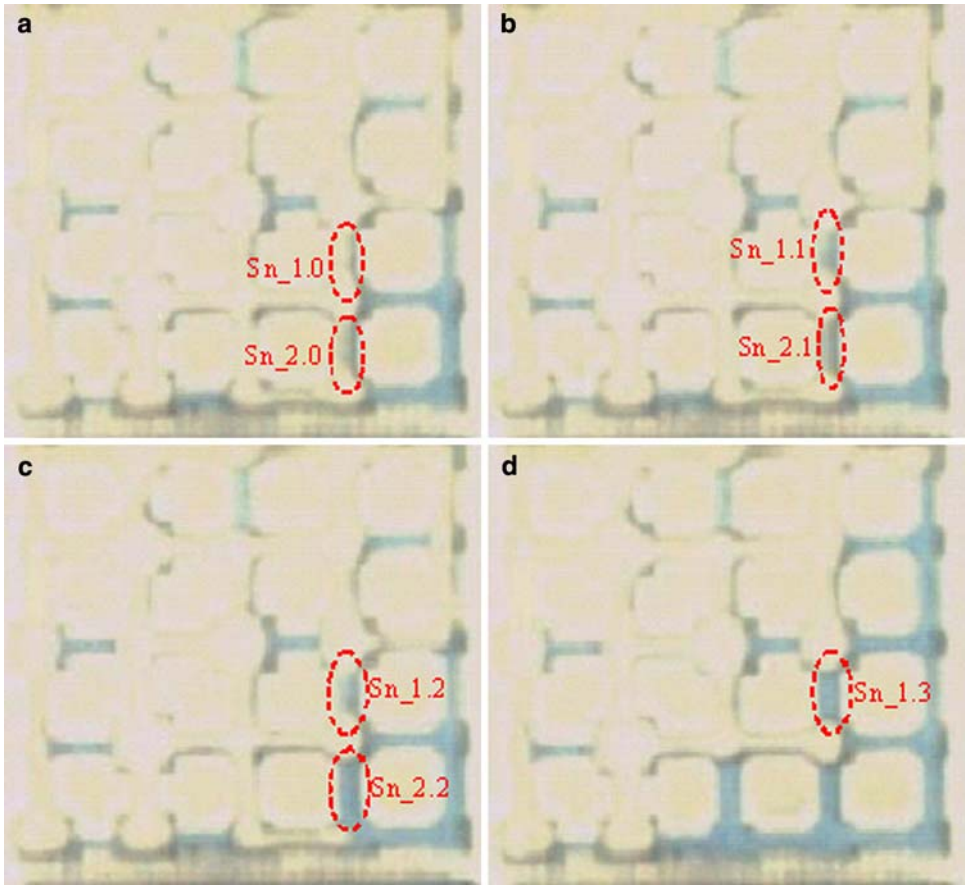

Fig. 6 **a** The beginning of the 12th stage of the imbibition **b** The 12th stage of the imbibition process **c** The 12th stage of the imbibition process **d** The end of the 12th stage of the imbibition process

Figure 7a–d shows the selected images in the 14th stage, where P_{ce} equals to 2.8 cmH_2O. The circled areas in the images demonstrate the detailed process of In imbibition and snap-off. Figure 7a is the starting image of the In imbibition and snap-off for the selected pores and throat. The sizes of 'I1_1.0', 'I1_2.0' and 'Sn_1.0' are 0.88, 0.72 and 0.42 mm, respectively. The computed P_{I1} for 'I1_1.j' and 'I1_2.j' are 2.97 and 3.28 cmH_2O, respectively. For the 'Sn_1.j', $P_{snap\text{-}off1}$ is 2.65 cmH_2O, while $P_{snap\text{-}off2}$ is 3.48 cmH_2O. $P_{snap\text{-}off1}$ is 0.15 cmH_2O lower than P_{ce}, while $P_{snap\text{-}off2}$ is 0.68 cmH_2O greater than P_{ce}.. Thus, the experimental snap-off capillary pressure is closer to the critical capillary pressure calculated by Hughes's equation in this stage.

'Sn_1.0' indicates the snap-off starting image at the selected throat. There is only one wetting throat close to 'Sn_1.0' as Fig. 7a shows. Because the upper and lower throats at 'I1_1.j' were wetted through the snap-off in the 12th stage, the 'I1_1.j' pore has a high possibility for producing I1 type imbibition, as the same figure shows. The meniscus in pore 'I1_1.0' was not stable as the capillary pressure decreased from the 12th stage to the 14th stage, causing the meniscus to collapse and wetting phase fluid to fill the 'I1_1.1' pore and its connected throat in Fig. 7b. The wetting phase fluid fills the 'I1_1.1' pore and its connecting throat when the I1 type imbibition and piston-type motion processes are all completed. Figure 7b shows that two of the four connecting throats of pore 'I1_2.1' are filled with wetting phase fluid, and the pore has a high possibility for I1 type imbibition if the throat 'Sn_1.1' is wetted. Figure 7c shows that the snap-off at throat 'Sn_1.2', the I1 type imbibition at pore 'I1_2.2' and the piston-type motion at the throat neighboring 'I1_2.2' are all completed.

The P_{I1} for 'I1_1.j' and 'I1_2.j' are 0.17 and 0.48 cmH_2O greater than P_{ce}, respectively. To produce I1 type imbibition in a pore, three connecting throats of the pore must be wetted. The fact that the experimental capillary pressure P_{ce} was close to the computed P_{In} at 'I1_1.j' indicates that Lenormand's estimation for the I1 type imbibition is accurate when enough surrounding throats of a pore are wetted. On the other hand, there was only one wetted throat for pore 'I1_2.j' in the beginning, as Fig. 7a shows. The capillary pressure must be smaller for the connecting throats to be wetted before I1 type imbibition occurs at pore 'I1_2.j'. Therefore, the difference between P_{ce} and P_{I1} is greater at 'I1_2.j' than at 'I1_1.j'. Computing the saturation increase using image processing shows that the contribution to the saturation increase is 15.3% by snap-off and 54.6% by I1 type imbibition and its associated piston-type motion in this stage.

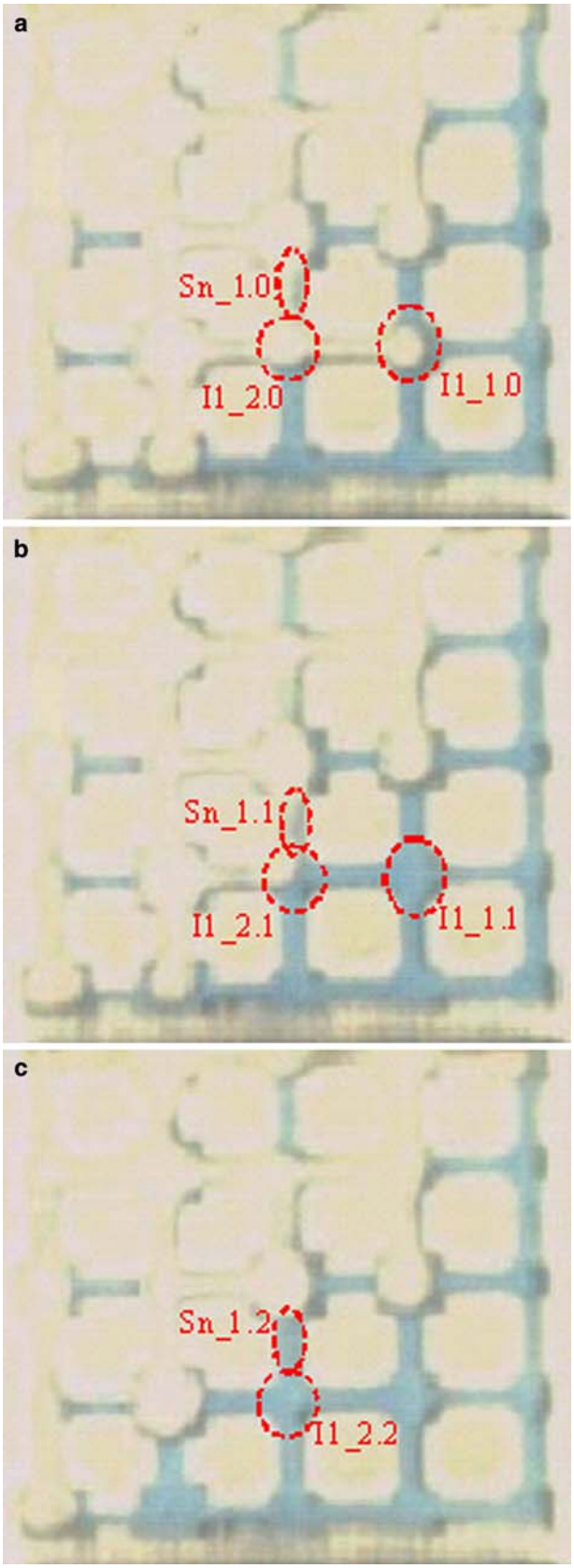

Fig. 7 **a** The 14th stage of the imbibition process **b** The 14th stage of the imbibition process **c** The end of the 14th stage of imbibition

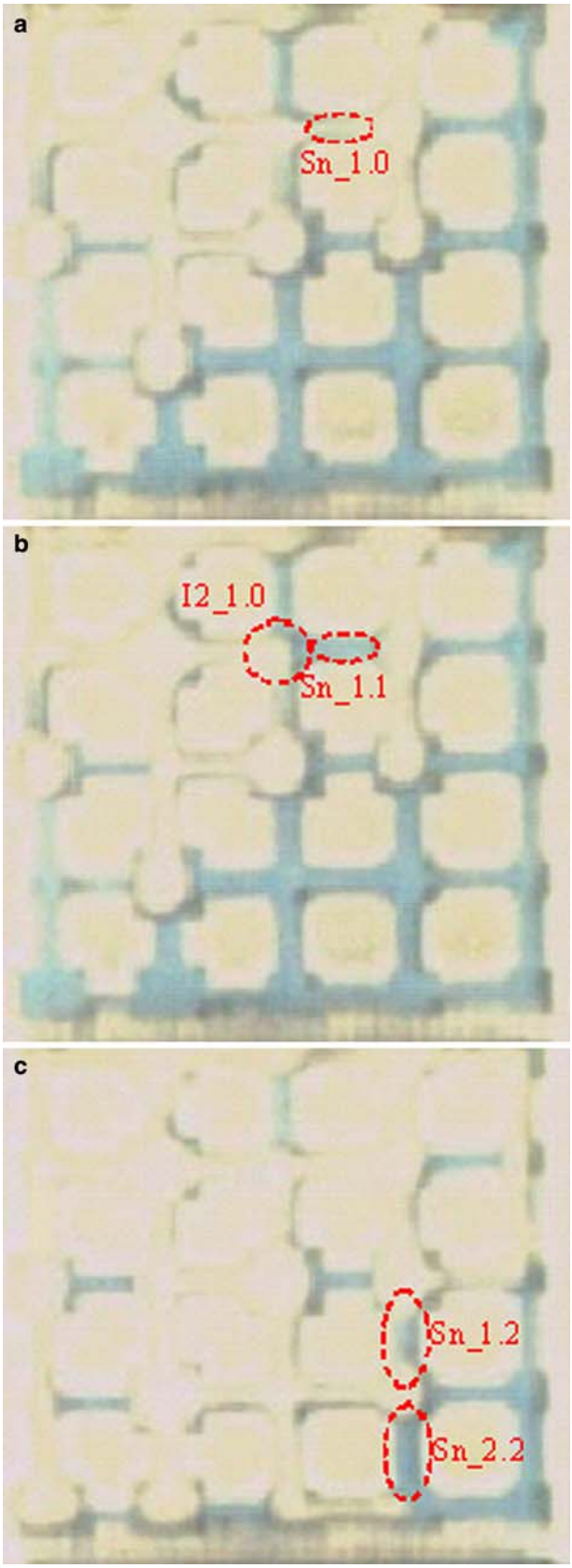

Fig. 8 **a** The 16th stage of the imbibition process **b** The 16th stage of the imbibition process **c** The 16th stage of the imbibition process

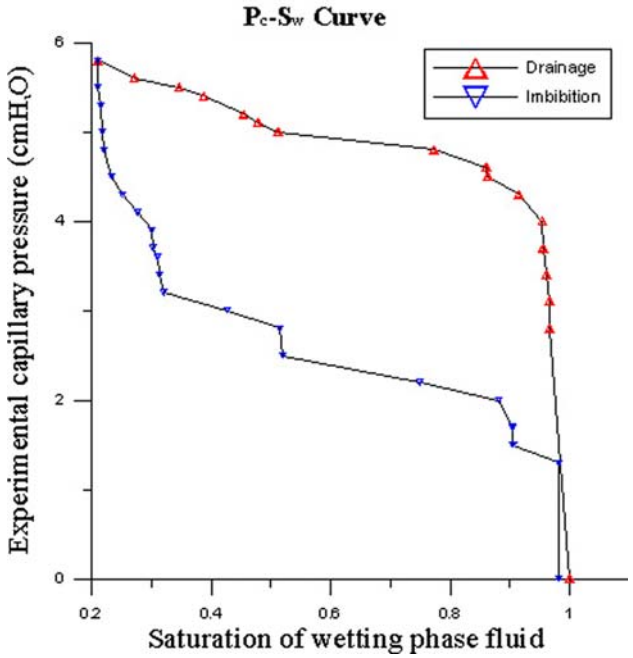

Fig. 9 The capillary pressure–saturation curve in the pore–throat network of the transparent micro model

Figure 8a–c shows selected images of the 16th stage, where the experimental P_{ce} was 2.2 cmH_2O. The size of 'I2_1.0' is 0.72 mm, and its estimated critical capillary pressure for producing the I2 type imbibition (P_{I2}) is 2.13 cmH_2O. Figure 8b shows that the two throats surrounding pore 'I2_1.0' become wetted before the I2 type imbibition occurs. The P_{ce} was close to the P_{I2}, indicating that Lenormand's estimation for I2 type imbibition is accurate when enough surrounding throats of a pore are wetted. Figure 8c indicates the I2 type imbibition is complete at 'I2_1.1'.

In type imbibition is the major displacement mechanism for wetting porous media, while snap-off can affect the occurrence of In type imbibitions. The experimental P_c–S_w curve (Fig. 9) shows the significant change for the saturation of wetting phase fluid ($S_{w)}$ when the In type imbibition occurs at $P_{ce} = 2.8$, 2.2 and 2.0 cmH_2O. Table 4 shows that the increase of the wetting phase fluid saturation during In type imbibition and its associated piston-type motion is 0.088, 0.229 and 0.131. These results imply that In type imbibition is the major displacement mechanism for the wetting phase fluid to invade the unsaturated pores and throats. Moreover, as mentioned above, before the In type imbibition of a pore can occur, enough surrounding throats must be wetted. For the pore–throat distribution applied in this study, snap-off can facilitate the occurrence of In type imbibition and its associated piston-type motion. Therefore, snap-off is an important displacement mechanism in facilitating the increase of the wetting phase fluid saturation in the imbibition process. Figure 10 summarizes the occurrence of displacement mechanisms and demonstrates that snap-off occurs before In type imbibitions.

Conclusion

This experimental study demonstrates that a transparent micro model can be a valuable tool to investigate the multiphase flow displacement at pore scale. The results of this experimental study show several important points.

Experimental images show that snap-off of a throat may occur without direct connection to other continuous wetted areas, and this implies the existence of corner flow. When more saturated pores or throats are positioned close to a throat, the critical snap-off capillary pressure for the throat estimated by Lenormand's formula is closer to the experimental value than that estimated by Hughes's formula. On the other hand, when few saturated pores or throats are close to a throat, Hughes's formula is more accurate. Further, the critical capillary pressures of I1 and I2 type imbibition estimated by Lenormand's formulas for a pore are closer to the experimental value when enough connecting throats were saturated.

Analysis of the saturation variation during the imbibition process shows that In type imbibition is the major displacement mechanism for wetting porous media in the imbibition process. However, before the In type imbibition of a pore can occur, there must be enough wetted throats

Table 4 The "imbibition process displacement mechanisms" statistics for the imbibition process in this experiment

	P_{ce} (cmH_2O)	S_w (%)	Increment of saturation	Saturation variation induced by snap-off	Saturation variation induced by I1 type imbibition and it's associated piston-type motion	Saturation variation induced by I2 type imbibition and it's associated piston-type motion
Stage 13	3	0.427	0.427			
Stage 14	2.8	0.514	0.088	0.013	0.048	
Stage 15	2.5	0.520	0.006			
Stage 16	2.2	0.749	0.229	0.014	0.138	0.049
Stage 17	2	0.881	0.131		0.072	0.057

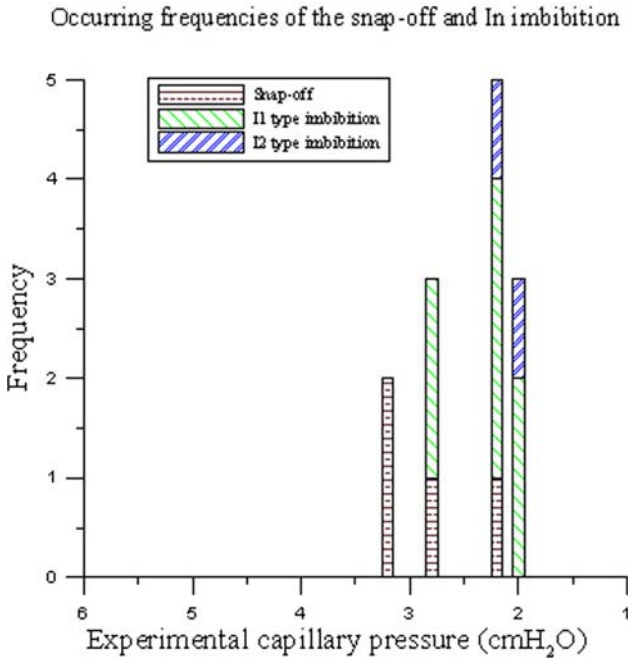

Fig. 10 Snap-off and In imbibition occurrence frequencies in imbibition process

surrounding the pore. For the pore–throat distribution applied in this study, the snap-off can facilitate the occurrence of In type imbibition and its associated piston-type motion. Therefore, snap-off is also an important displacement mechanism in facilitating the increase of the wetting phase fluid saturation in the imbibition process.

Acknowledgments The authors would like to thank the National Science Council of the Republic of China, Taiwan, for financially supporting this research under Contract No. 96-2221-E-009-090.

References

Blunt MJ (1997) Effects of heterogeneity and wetting on relative permeability using pore level modeling. SPE J 2:70–87

Blunt M, King MJ, Scher H (1992) Simulation and theory of two-phase flow in porous media. Phy Rev A 46(12):7680–7699

Chang LC, Chen HH, Shan HY, Tsai JP (2008) Effect of connectivity and wettability on the relative permeability of NAPLs. Environ Geol 56:1437–1447. doi:10.1007/s00254-008-1238-8

Dodd CG, Kiel OG (1959) Evaluation of Monte Carlo methods in studying fluid–fluid displacements and wettability in porous rocks. J Phys Chem 63:1646–1652

Hughes RG (1998) Network modeling of imbibition in fractured porous media. PhD, Stanford University, Stanford, CA

Hughes RG, Blunt MJ (2000) Pore scale modeling of rate effects in imbibition. Transport Porous Med 40:295–322

Hughes RG, Blunt MJ (2001) Network modeling of multiphase flow in fractures. Adv Water Resour 24:408–421

Ioannidis MA, Chatzis I (1993) A mixed-percolation model of capillary hysteresis and entrapment in mercury porosimetry. J Colloid Interf Sci 161:278–291

Ioannidis MA, Chatzis I, Payatakes AC (1991) A mercury porosimeter for investigating capillary phenomena and microdisplacement mechanisms in capillary networks. J Colloid Interf Sci 143(1)

Jerauld GR, Salter SJ (1990) The effect of pore-structure on hysteresis in relative permeability and capillary pressure: pore-level modeling. Transp Porous Media 5:103–151

Kawanishi T, Hayashi Y, Roberts PV, Blunt MJ (1998) Fluid-fluid interfacial area during two and three phase fluid displacement in porous media: a network study. In: Proceedings of the international conference on groundwater quality: remediation and protection, Tubingen, Germany, September, pp 89–96

Lenormand R, Zarcone C (1984b) Role of roughness and edges during imbibition in square capillaries, Paper SPE 13264, Proc paper presented at the 59th SPE annual technical conference and exhibition, Houston, TX, September, 16–19, 1984

Lenormand R, Zarcone C, Sarr (1983) A Mechanisms of the displacement of one fluid by another in a network of capillary ducts. J Fluid Mech 135:337–353

Li Y, Wardlaw NC (1986) The influence of wettability and critical pore-throat size ration on snap-off. J Colloid Interf Sci 109(2):461–472

Mahmud WM, Nguyen VH (2006) Effects of snap-off in imbibition in porous media with different spatial correlations. Transp Porous Med 64:279–300

Mogensen K, Stenby E (1998) A dynamic pore-scale model of imbibition. Paper SPE 39658. Paper presented at the improved oil recovery symposium, Tulsa, OK, pp 19–22

Reeves PC (1997) The development of pore-scale network models for the simulation of capillary pressure-saturation-interfacial area-relative permeability relationships in multi-fluid porous media. PhD, Princeton University, Princeton, NJ

Vidales AM, Riccardo JL, Zgrablich G (1998) Pore-level modelling of wetting on correlated porous media. J Phys D Appl Phys 31:2861–2868

Wardlaw NC, Taylor RP (1976) Mercury capillary pressure curves and the interpretation of pore structure and capillary behaviour in reservoir rocks. Bull Can Petrol Geol 24:225–262